

KLF4 overexpression protects against complement-mediated endothelial injury in transplant-associated thrombotic microangiopathy

Shuhui Jiang,^{1-3*} Jiaqian Qi,^{1-3*} Tingting Pan,^{1-3*} Zhenzhen Yao,¹⁻³ Siyi Lu,¹⁻³ Yifei Han,¹⁻³ Depei Wu¹⁻⁴ and Yue Han¹⁻⁴

¹National Clinical Research Center for Hematologic Diseases, Jiangsu Institute of Hematology, The First Affiliated Hospital of Soochow University; ²Institute of Blood and Marrow Transplantation, Collaborative Innovation Center of Hematology, Soochow University; ³Key Laboratory of Thrombosis and Hemostasis of Ministry of Health and ⁴State Key Laboratory of Radiation Medicine and Protection, Soochow University, Suzhou, China

*SJ, JQ and TP contributed equally as first authors.

Correspondence: D. Wu
drwudepei@163.com

Y. Han
hanyue@suda.edu.cn

Received: March 4, 2025.

Accepted: July 28, 2025.

Early view: August 7, 2025.

<https://doi.org/10.3324/haematol.2025.287676>

©2026 Ferrata Storti Foundation

Published under a CC BY-NC license



Supplementary material

Supplementary methods

Definition of TA-TMA

According to the published diagnostic criteria proposed in 2023,¹ TA-TMA is diagnosed when at least four of the following seven features are documented on two occasions within a 14-day window:

1. **Anemia**—failure to attain transfusion independence after neutrophil engraftment, a ≥ 1 g/dL drop in hemoglobin, or new transfusion dependence.
2. **Thrombocytopenia**—failure to achieve platelet engraftment, higher-than-expected platelet transfusion requirements, refractoriness to platelet transfusion, or a $\geq 50\%$ decline in baseline platelet count after full engraftment.
3. **Elevated lactate dehydrogenase (LDH)**—serum LDH above the upper limit of normal (ULN).
4. **Schistocytosis**—presence of schistocytes on blood smear.
5. **Hypertension**—new-onset or worsening hypertension.
6. **Elevated soluble C5b-9**—levels exceeding the ULN.
7. **Proteinuria**—random urine protein-to-creatinine ratio (rUPCR) ≥ 1 mg/mg.

Enzyme-linked immunosorbent assay

Human plasma levels of complement components (C3b and sC5b-9) (Novus, #NBP2-60553, CV% < 9.9%, detect range [0.156–5] ng/mL; Novus, #NBP2-66708, CV% < 5.07%, detect range [31.25–2000] ng/mL), inflammatory/thrombotic endothelial factors (ICAM-1,

VCAM-1, ST2, and PAI-1) (Cusbio, #CSB-E04574h, CV% < 10%, detect range [0.78–50] ng/mL; Cusbio, #CSB-E04753h, CV% < 10%, detect range [1.563–100] ng/mL; Cusbio, #CSB-E13789h, CV% < 10%, detect range [0.312–20] ng/mL; Proteintech, #KE00109, CV% < 2.6%, detect range [0.313–20] ng/mL) and KLF4 (Cusbio, #CSB-EL012394HU, CV% < 10%, detect range [18.75–1200] pg/mL) were measured using commercial enzyme-linked immunosorbent assay (ELISA) kits according to the manufacturers' instructions. Additionally, mouse plasma levels of sC5b-9 (Krishgen, #KLM0637, CV% < 10%, detect range [1.562–100] ng/mL), ICAM-1 (Proteintech, #KE10063, CV% < 2.7%, detect range [15.6–1000] pg/mL), VCAM-1 (Cusbio, #CSB-E04754m, CV% < 10%, detect range [39.062–2500] pg/mL) and PAI-1 (Cusbio, #CSB-E07947m, CV% < 10%, detect range [0.9–60] ng/mL) were assessed via ELISA.

Cell culture and treatment

Human umbilical vein endothelial cells (HUVECs; ATCC) were used to establish the complement-adherent in-vitro model as previously described.² To stimulate KLF4, cells were pre-treated with the small-molecule activator APTO-253 (MCE, #HY-16291) at 10 μ M for 24 h before evaluating complement deposition and endothelial-injury markers.

To generate HUVEC cell lines with either KLF4 overexpression or CD46 knockdown, a lentiviral-mediated approach was employed. A lentiviral vector (pCDH-SFFV-IRES-EGFP) encoding full-length human KLF4 (designated OEKLF4) and its control lentiviral vector (designated PCDH) were purchased from General Biol Ltd. Additionally, a pLKO.1-CMV-

copGFP-PURO vector for CD46 knockdown (designated ShCD46) and its corresponding control vector (designated PLKO.1) were obtained from Beijing Tsingke Biotech Ltd.

Flow cytometry

A five-color flow cytometric assay³ (phycoerythrin [PE]-conjugated anti-CD45, BioLegend, #982322; PE-cyanine [Cy7]-conjugated anti-CD34, BioLegend, #343515; allophycocyanin [APC]-Cy7-conjugated anti-CD146, BioLegend, #361041; APC-conjugated anti-CD133, BioLegend, #372805; brilliant violet-421-conjugated anti-CD106, BioLegend, #305815) was employed to detect and characterize CECs and their subpopulations in patients' peripheral blood. mCECs were defined as CD34⁺/CD45⁻/CD133⁻/CD146⁺; EPCs were identified as CD34⁺/CD45⁻/CD146⁺/CD133⁺; rCECs were CD34⁺/CD45⁻/CD146⁺/CD106⁻; and aCECs were CD34⁺/CD45⁻/CD146⁺/CD106⁺.

Flow cytometry was also used to assess the deposition of C3 and C5b-9 on HUVECs. Cells were incubated with fluorescein isothiocyanate (FITC)-conjugated anti-C3 antibody (Abcam, #ab4212) or anti-C5b-9 antibody (Abcam, #ab55811), followed by Alexa Fluor 647-conjugated goat anti-rabbit IgG H&L (Beyotime, #A0468). For HUVECs transduced with various lentiviral vectors, C5b-9 deposition was measured as above, whereas C3 deposition was detected using an APC-conjugated anti-C3 antibody (BioLegend, #846105).

Apoptosis was evaluated using the Annexin V-APC/7-AAD Apoptosis Kit (MultiSciences, #AP105) according to the manufacturer's instructions, followed by flow cytometric analysis.

Western blot analysis

Samples were subjected to immunoblotting using primary antibodies against human KLF4 (Abcam, #ab215036), CD46 (Abcam, #ab108307), C3 (Abcam, #ab181147), C5 (Proteintech, #66634-1-Ig), C4 (Proteintech, #22233-1-AP), CFB (Proteintech, #10170-1-AP), MBL2 (Invitrogen, #PA5-106674), C1QA (Proteintech, #67063-1-Ig) or β -actin (Proteintech, #66009-1-Ig), followed by corresponding species-specific secondary antibodies (Proteintech, #SA00001-1; Proteintech, #SA00001-2). This method enabled the assessment of protein levels for various complement components.

Quantitative real-time PCR

Quantitative real-time PCR (qPCR) was performed to assess the expression levels of various inflammatory and thrombotic endothelial genes, using primer sequences provided in Table S4. Relative gene expression was calculated using the comparative $2^{-\Delta\Delta Ct}$ method, normalized to the corresponding housekeeping gene.

Immunofluorescence staining

The cells treated with TA-TMA or control plasma were fixed with 4% paraformaldehyde PBS solution and permeabilized with 0.5% Triton X-100. After the cells were blocked with 10% normal goat serum for 1h, they were incubated with the same primary antibodies as in the Western blot analysis at 4°C overnight. Then they were stained with Alexa Fluor 647–conjugated goat anti-rabbit IgG H&L (Beyotime, #A0468) or Alexa Fluor 647 goat anti-

mouse IgG H&L (CST, #4410) for 2 h, followed by DAPI (Beyotime, #C1002) for 15 min at room temperature. Frozen mouse kidney sections were stained with anti-C3 (Abcam, #ab11862), anti-C5b-9 (Santa Cruz, #sc-66190), or anti-CD31 (Invitrogen, #PA5-32321) antibodies. Confocal images were acquired using a Leica inverted multiphoton laser scanning microscope. Immunofluorescence staining provides a direct visual representation of complement activation in cells and tissues.

Transendothelial electrical resistance and cell permeability

Cells were seeded onto 24-well Millicell inserts (pore size 0.4 μm , LABSELECT) and cultured until confluent. Transendothelial electrical resistance (TEER) was determined using a Millicell-ERS apparatus equipped with an electrode, and the change in resistance (ΔTEER) was calculated before and after plasma exposure, expressed as a percentage decrease from baseline. After 24h of plasma exposure, FITC-dextran (Sigma-Aldrich, #46944) was added to the apical chamber. Subsequently, 50 μL of medium from the lower chamber was transferred to a 96-well assay plate and its fluorescence intensity read at excitation/emission wavelengths of 485/540 nm using a BioTek plate reader.

CUT&Tag

CUT&Tag analysis was performed on KLF4-overexpressing HUVECs and control HUVECs, each exposed to TA-TMA plasma for 12 hours, by Jiayin Biotechnology Ltd. (Shanghai, China), following previously described protocols. Nuclei (5×10^5 per sample) were washed twice in wash buffer (20 mM HEPES, pH 7.5; 150 mM NaCl; 0.5 mM spermidine; $1 \times$

protease-inhibitor cocktail). Each suspension was combined with 10 μ L concanavalin A-coated magnetic beads (Bangs Laboratories) and incubated for 10 min at room temperature (RT). After removing unbound material, bead-bound nuclei were resuspended in DIG wash buffer (20 mM HEPES, pH 7.5; 150 mM NaCl; 0.5 mM spermidine; 1 \times protease-inhibitor cocktail; 0.05% digitonin; 2 mM EDTA) and incubated overnight at 4°C with rotation with either anti-KLF4 antibody (Bio-Techne, #AF3640) or normal goat IgG (Bio-Techne, #AB-108-C). Following magnetic separation, nuclei were incubated for 60 min at RT with anti-goat IgG secondary antibody (Biodragon, #BF02015) diluted in DIG wash buffer. After three washes in DIG wash buffer, nuclei were incubated for 1 h at RT with a pA-Tn5 adapter complex (1:100) prepared in Dig-med buffer (20 mM HEPES, pH 7.5; 300 mM NaCl; 0.5 mM spermidine; 1 \times protease-inhibitor cocktail; 0.01% digitonin). Samples were washed three times in Dig-med buffer, resuspended in tagmentation buffer (Dig-med + 10 mM MgCl₂), and tagmented for 1 h at 37°C. DNA was extracted by phenol-chloroform-isoamyl-alcohol and ethanol-precipitated, then PCR-amplified to generate sequencing libraries. Library size was verified on an Agilent 4200 TapeStation, and 150-bp paired-end sequencing was performed on an Illumina NovaSeq 6000. After quality control, reads were aligned to the reference genome with BWA, peaks were called with MACS2 (q < 0.05), annotated using ChIPseeker, and differential binding was assessed with DESeq2 (|fold-change| \geq 2, p < 0.05). Chromosomal distributions of KLF4 binding sites were visualized with the RIdeograms package.

To identify specific transcription factor binding sites within the promoter region of our gene

of interest, we first employed the ‘Jaspar’ package, which provides a comprehensive database of position weight matrices (PWMs) for diverse transcription factors [PMID: 37962376]. We extracted the genomic sequence corresponding to the upstream regulatory region and imported these sequences into Jaspar for motif scanning. This process yielded a set of putative KLF4-binding motifs, each associated with a predicted binding probability.

Subsequently, we utilized the ‘Basenji’ deep-learning framework to evaluate the functional significance of these potential regulatory elements. Basenji predicts gene expression by integrating long-range regulatory information through its multi-scale convolutional neural network architecture. Specifically, the model processes extended DNA sequences, often spanning tens to hundreds of kilobases, allowing it to capture enhancer–promoter interactions and distal regulatory cues that might influence transcriptional output [PMID: 32943643].

Within this computational platform, we performed *in silico* mutagenesis by systematically “knocking out” each putative KLF4-binding motif—replacing or removing the core nucleotides of the predicted site—while preserving the rest of the sequence context. Basenji then recomputed the predicted expression level for each altered sequence, providing a quantitative measure of the potential impact of each site’s disruption. This step was crucial for identifying which motifs are most likely to contribute significantly to gene regulation.

By integrating the results from Jaspar motif identification with Basenji's predicted expression changes, we gained a clearer understanding of how KLF4 binding sites within the promoter region may shape transcriptional regulation and, ultimately, downstream biological processes.

RNA sequencing

Two distinct cell populations, hCECs and aHUVCEs (n = 3 biological replicates per group), underwent total RNA extraction using a column-based purification kit, according to the manufacturer's guidelines. KLF4-overexpressing HUVECs and control HUVECs were each incubated with TA-TMA plasma for 12 hours (n = 3 per group), after which RNA-seq was performed. Library preparation, sequencing, and data analysis were carried out by Jiayin Biotechnology Ltd. (Shanghai, China), following previously described protocols. Differentially expressed genes (DEGs) were identified using the DESeq2 package ($|\text{fold change}| \geq 1.2$, $p < 0.05$). KEGG analysis was conducted, and the results were visualized using the OmicShare tool, an online data analysis platform.

Transfection and luciferase assays

Human CD46 reporter constructs were transfected into HEK 293T cells using FuGENE®6 Transfection Reagent (Promega, #E2691) according to the manufacturer's instructions. KLF4 or a control vector was co-transfected concurrently. A Renilla luciferase plasmid served as the internal control. After 48 hours, cells were lysed and analyzed with a luciferase assay (Promega, #E1910). The results were expressed as normalized fold

changes relative to controls. These luciferase assays verified the relationship between KLF4 expression and target gene transcription.

Animal treatment

Female 8-week-old C57BL/6J and BALB/C mice (Charles River Laboratories) were maintained in a specific-pathogen-free (SPF) facility at Soochow University.

To establish a hematopoietic stem cell transplantation model, BALB/C mice received a single lethal dose of total body X-ray irradiation (650 cGy) and were then transplanted with 1×10^7 C57BL/6J bone marrow cells via tail vein injection.⁴

To induce KLF4 expression, APTO-253 (MCE, #HY-16291) was administered by oral gavage twice daily at 5 mg/kg, dissolved in DMSO (Sigma-Aldrich, D4540), on post-transplant days +6, +8, +10, +12, and +14. Vehicle-treated animals received equivalent volumes of the solvent as controls.

We overexpressed KLF4 *in vivo* using a commercially available cationic polymer transfection reagent (*in vivo*-jetPEI®, Polyplus Transfection, #101000030). In brief, 30 µg of mKLF4 plasmid or the corresponding control vector (pcDNA3.1) was diluted in 200 µL of 5% glucose solution and mixed with *in vivo*-jetPEI® at the recommended ionic balance (N/P = 6-8). To achieve optimal KLF4 overexpression, the plasmid/ *in vivo*-jetPEI® mixture was administered via i.v. injection on days +12 and +14 post-transplantation to BALB/C

mice that had undergone allo-HSCT.

Pravastatin (20 mg/kg in 0.9% saline) was administered via oral gavage daily from post-transplantation days +8 to +14, while vehicle-treated groups received equivalent volumes of 0.9% saline through the same administration route and schedule during this period.

Then immunoblotting was performed on the kidney using an antibody against mouse KLF4 (Abcam, #ab214666) to validate its expression.

To reproduce TA-TMA pathology in vivo, we applied the dimethyloxalyglycine (DMOG) protocol previously optimized by our group.² Starting on day +15 after allo-HSCT, mice received daily intraperitoneal injections of DMOG (800 mg/kg; MCE, HY-15893) for two consecutive days, while control animals received equal volumes of 0.9% saline vehicle.

Statistics

Statistical analyses were conducted using GraphPad Prism 9.0 and SPSS 27.0 software. The Mann-Whitney *U* test (continuous variables) and chi-square test or Fisher's exact test (categorical variables) were used to estimate significant differences in baseline characteristics between the TA-TMA and control groups. Differences between two groups were evaluated using two-tailed Student's *t*-tests. For comparisons involving more than two groups, one-way analysis of variance (ANOVA) followed by Bonferroni's post-hoc test was employed. Survival incidence was assessed by the Kaplan-Meier method and the log-

rank test. Datas are described using mean \pm standard deviation, while some datas are presented as median and interquartile range. A p-value < 0.05 was considered statistically significant.

References

1. Schoettler ML, Carreras E, Cho B, et al. Harmonizing Definitions for Diagnostic Criteria and Prognostic Assessment of Transplantation-Associated Thrombotic Microangiopathy: A Report on Behalf of the European Society for Blood and Marrow Transplantation, American Society for Transplantation and Cellular Therapy, Asia-Pacific Blood and Marrow Transplantation Group, and Center for International Blood and Marrow Transplant Research. *Transplant Cell Ther* 2023; 29(3): 151-163.
2. Qi J, Pan T, You T, et al. Upregulation of HIF-1 α contributes to complement activation in transplantation-associated thrombotic microangiopathy. *Br J Haematol* 2022; 199(4): 603-615.
3. Zhou F, Zhou Y, Yang M, Wen J, Dong J, Tan W. Optimized multiparametric flow cytometric analysis of circulating endothelial cells and their subpopulations in peripheral blood of patients with solid tumors: a technical analysis. *Cancer Manag Res* 2018; 10: 447-464.
4. Cai Y, Ma S, Liu Y, et al. Adoptively transferred donor IL-17-producing CD4(+) T cells augment, but IL-17 alleviates, acute graft-versus-host disease. *Cell Mol Immunol* 2018; 15(3): 233-245.

Table S1 Clinical and laboratory parameters in TA-TMA patients and controls at sampling.

	Ctrl (n = 20)	TA-TMA (n = 20)	p-value
Median HGB, g/L (IQR)	92, 72.5-99.75	59, 52-69	< 0.0001
Median PLT, ×10 ⁹ /L (IQR)	73.5, 43-117.5	12.5, 7-17.25	< 0.0001
Median LDH, U/L (IQR)	251.5, 208.0-339.0	654.0, 492.0-1076	< 0.0001
Median sC5b-9, ng/ml (IQR)	485.3, 443.0-564.3	1139, 754.1-1461	< 0.0001
rUPCR, n (%)			0.002
≥1 mg/mg	4 (20)	15 (75)	
<1 mg/mg	16 (80)	5 (25)	
Schistocytes, n (%)			< 0.001
Yes	1 (5)	12 (60)	
No	19 (95)	8 (40)	
Hypertension, n (%)			< 0.001
Yes	3 (15)	15 (75)	
No	17 (85)	5 (25)	

Abbreviations: HGB, hemoglobin; PLT, platelet; LDH, lactate dehydrogenase; rUPCR, random urine protein-to-creatinine ratio; IQR, interquartile range.

Table S2 Comparison of the numbers of CECs and their subpopulations in TA-TMA patients and controls.

Subpopulations	Ctrl (n = 10)	TA-TMA (n = 10)	p-value
Total cells	1×10^6	1×10^6	
mCECs (mean \pm standard deviation)	22.5 ± 7.706	88.5 ± 38.31	< 0.001
rCECs (mean \pm standard deviation)	24 ± 8.969	92.5 ± 40.24	< 0.001

Abbreviations: CECs, circulating endothelial cells; mCECs, mature ECs; rCECs, resting CECs.

Table S3 The predicted binding sites of KLF4 to CD46 as determined by CUT&Tag analysis

group	group_name	start	end	width	strand	score
1	NA	45	56	12	+	16.9044
1	NA	138	149	12	+	16.9044
2	NA	25	36	12	+	10.4034
2	NA	50	61	12	+	10.4034
3	NA	55	66	12	-	15.3195
3	NA	92	103	12	-	15.3195
3	NA	277	288	12	-	15.3195
4	NA	137	148	12	+	11.1982
5	NA	154	165	12	+	16.8562
6	NA	31	42	12	+	18.3429
6	NA	198	209	12	+	18.3429
7	NA	183	194	12	+	13.3239
8	NA	9	20	12	-	18.7868
9	NA	26	37	12	-	14.4497
10	NA	89	100	12	-	13.337
11	NA	11	22	12	+	10.7834
12	NA	100	111	12	+	18.0782
12	NA	309	320	12	+	18.0782
13	NA	169	180	12	+	15.1813
14	NA	55	66	12	+	7.28188
15	NA	290	301	12	-	17.268
16	NA	361	372	12	-	11.9243
16	NA	402	413	12	-	11.9243
17	NA	116	127	12	-	8.83229
18	NA	57	68	12	-	16.7749
19	NA	110	121	12	+	19.7101
20	NA	118	129	12	-	13.1542
21	NA	180	191	12	+	14.1056
22	NA	9	20	12	+	14.4222
23	NA	84	95	12	-	17.1012
24	NA	104	115	12	+	17.9629
25	NA	146	157	12	+	12.6989
26	NA	37	48	12	-	14.6597
27	NA	270	281	12	-	12.06
28	NA	179	190	12	-	16.2173
29	NA	249	260	12	+	18.2715
30	NA	72	83	12	-	17.2163
31	NA	179	190	12	-	13.8631
32	NA	55	66	12	+	17.2852
33	NA	225	236	12	+	16.4033
34	NA	173	184	12	+	17.704
35	NA	166	177	12	-	13.2508
36	NA	156	167	12	+	16.7067
37	NA	276	287	12	+	13.4827
38	NA	194	205	12	-	15.3495
39	NA	31	42	12	+	13.0741
40	NA	345	356	12	+	19.4453
41	NA	137	148	12	-	13.0267
42	NA	370	381	12	-	18.0782
43	NA	82	93	12	-	12.2288
44	NA	69	80	12	-	17.8694
45	NA	388	399	12	-	17.6981
46	NA	98	109	12	+	17.9128
47	NA	79	90	12	+	11.6202
48	NA	125	136	12	-	11.5453
49	NA	21	32	12	-	16.4033
50	NA	21	32	12	-	17.8694
51	NA	20	31	12	-	19.28

52	NA	41	52	12	-	17.8694
53	NA	54	65	12	-	11.7827
54	NA	31	42	12	+	16.6595
55	NA	17	28	12	+	18.0782
56	NA	73	84	12	-	15.4942
57	NA	16	27	12	+	17.9629
58	NA	101	112	12	-	18.5362
59	NA	4	15	12	-	9.85658
60	NA	36	47	12	-	16.1222
61	NA	102	113	12	+	14.8721
62	NA	179	190	12	-	13.9973
63	NA	75	86	12	+	12.446
64	NA	204	215	12	-	17.7204
65	NA	213	224	12	+	19.8254
66	NA	132	143	12	-	14.3932
67	NA	281	292	12	+	16.9052
68	NA	79	90	12	-	15.4119
69	NA	149	160	12	-	13.1082
70	NA	91	102	12	+	12.6069
71	NA	14	25	12	-	17.9629
71	NA	19	30	12	-	17.9629
72	NA	74	85	12	+	11.7078
73	NA	248	259	12	+	13.4533
74	NA	164	175	12	-	13.7287
75	NA	73	84	12	+	12.4342
76	NA	19	30	12	+	17.6481
77	NA	142	153	12	-	13.2277
78	NA	53	64	12	-	15.9592
79	NA	515	526	12	+	16.3782
80	NA	111	122	12	+	17.9629
80	NA	116	127	12	+	17.9629
81	NA	85	96	12	+	16.3948
82	NA	175	186	12	+	16.9044
83	NA	31	42	12	-	17.6981
83	NA	49	60	12	-	17.6981
83	NA	184	195	12	-	17.6981
83	NA	240	251	12	-	17.6981
84	NA	171	182	12	-	16.4761
85	NA	112	123	12	-	10.3143
86	NA	44	55	12	+	14.9002
87	NA	11	22	12	-	10.2666
88	NA	57	68	12	-	19.4453
89	NA	357	368	12	-	17.9629
90	NA	165	176	12	+	12.9305
91	NA	185	196	12	+	17.0396
92	NA	92	103	12	-	7.65363
93	NA	20	31	12	+	12.946
94	NA	55	66	12	-	18.5221
95	NA	185	196	12	-	11.3518
96	NA	48	59	12	+	15.3022
96	NA	211	222	12	+	15.3022
97	NA	309	320	12	-	17.6981
98	NA	78	89	12	+	8.7267
99	NA	258	269	12	-	17.8694
100	NA	134	145	12	+	10.9219
101	NA	206	217	12	-	16.5761
102	NA	24	35	12	-	17.2852
103	NA	289	300	12	-	11.9885
104	NA	121	132	12	-	11.5947
105	NA	23	34	12	-	16.668
106	NA	230	241	12	-	19.8254

107	NA	221	232	12	-	18.363
108	NA	4	15	12	-	13.7436
108	NA	44	55	12	-	13.7436
108	NA	84	95	12	-	13.7436
109	NA	14	25	12	-	16.92
110	NA	145	156	12	-	14.6762
111	NA	52	63	12	-	18.9163
112	NA	29	40	12	-	14.5707
113	NA	512	523	12	-	19.0152
114	NA	41	52	12	+	13.7385
115	NA	341	352	12	-	14.9595
116	NA	59	70	12	+	14.6795
117	NA	87	98	12	+	16.3541
118	NA	98	109	12	+	16.5243
119	NA	210	221	12	+	17.0596
120	NA	292	303	12	-	16.7119
121	NA	36	47	12	-	13.729
122	NA	194	205	12	+	14.5392
123	NA	15	26	12	+	10.8301
124	NA	274	285	12	+	11.7554
125	NA	123	134	12	-	17.1558
126	NA	172	183	12	+	18.1505
127	NA	97	108	12	-	17.5131
128	NA	117	128	12	+	18.0101
129	NA	142	153	12	+	13.2339
130	NA	5	16	12	-	19.8254
131	NA	94	105	12	-	18.9163
132	NA	23	34	12	+	16.7757
132	NA	79	90	12	+	16.7757
133	NA	247	258	12	+	11.0513
133	NA	295	306	12	+	11.0513
133	NA	395	406	12	+	11.0513
133	NA	421	432	12	+	11.0513
134	NA	5	16	12	+	9.30415
134	NA	31	42	12	+	9.30415
134	NA	55	66	12	+	9.30415
135	NA	175	186	12	+	17.6481
136	NA	268	279	12	-	18.0782
136	NA	352	363	12	-	18.0782
137	NA	6	17	12	+	18.3232
138	NA	82	93	12	-	19.3953
139	NA	49	60	12	-	17.8694
139	NA	218	229	12	-	17.8694
140	NA	576	587	12	+	16.6881
141	NA	44	55	12	-	18.0782
142	NA	193	204	12	-	18.142
143	NA	258	269	12	-	16.4899
144	NA	51	62	12	-	14.1003
145	NA	227	238	12	-	20.0901
146	NA	12	23	12	+	16.7119
147	NA	38	49	12	-	15.1
148	NA	150	161	12	+	16.8562
148	NA	33	44	12	-	16.8562
149	NA	199	210	12	-	13.8309
150	NA	4	15	12	-	18.5221
151	NA	51	62	12	+	12.5379
152	NA	21	32	12	+	11.2587
153	NA	12	23	12	-	15.129
154	NA	688	699	12	-	18.0782
155	NA	348	359	12	-	19.8254
156	NA	34	45	12	-	18.9163

157	NA	444	455	12	-	18.3429
157	NA	513	524	12	-	18.3429
158	NA	59	70	12	-	18.1341
158	NA	298	309	12	-	18.1341
159	NA	36	47	12	-	19.8254
160	NA	252	263	12	-	13.3511
161	NA	275	286	12	+	18.0782
162	NA	79	90	12	-	19.8254
163	NA	179	190	12	-	16.8562
164	NA	158	169	12	+	19.8254
165	NA	113	124	12	+	16.668
167	NA	138	149	12	+	8.07664
168	NA	108	119	12	-	8.52668
169	NA	235	246	12	+	18.363
170	NA	342	353	12	-	16.789
171	NA	130	141	12	-	18.0782
171	NA	162	173	12	-	18.0782
172	NA	147	158	12	-	16.8562
173	NA	163	174	12	+	18.0782
174	NA	150	161	12	-	13.2035
175	NA	17	28	12	-	18.1341
176	NA	31	42	12	-	18.3429
176	NA	112	123	12	-	18.3429
177	NA	227	238	12	-	18.0782
178	NA	48	59	12	+	13.3761
179	NA	286	297	12	-	16.9516
180	NA	254	265	12	-	18.3902
181	NA	173	184	12	+	17.0868
182	NA	335	346	12	+	17.8694
183	NA	5	16	12	+	16.4761
183	NA	249	260	12	+	16.4761
184	NA	102	113	12	-	17.3
185	NA	333	344	12	+	12.1125
186	NA	88	99	12	+	17.9629
187	NA	193	204	12	-	13.5992
188	NA	95	106	12	-	18.5362
189	NA	137	148	12	-	18.7868
190	NA	91	102	12	-	14.9507
191	NA	54	65	12	-	12.8836
192	NA	159	170	12	+	15.3022
193	NA	278	289	12	-	16.3511
194	NA	84	95	12	+	17.9629
195	NA	46	57	12	+	12.7743
195	NA	146	157	12	+	12.7743
196	NA	112	123	12	-	14.7971
197	NA	546	557	12	+	19.3953
198	NA	473	484	12	+	18.0782
199	NA	7	18	12	-	16.4033
200	NA	152	163	12	-	11.1474
201	NA	58	69	12	-	11.5631
202	NA	24	35	12	+	11.9322
203	NA	169	180	12	-	15.6823
204	NA	73	84	12	+	14.6544
205	NA	140	151	12	+	18.363
206	NA	169	180	12	-	13.3486
207	NA	549	560	12	-	15.1813
208	NA	47	58	12	-	14.1406
209	NA	108	119	12	+	16.4033
210	NA	22	33	12	+	18.0782
211	NA	54	65	12	+	12.2925
212	NA	67	78	12	-	11.7697

213	NA	50	61	12	+	13.0882
214	NA	251	262	12	+	16.8408
215	NA	63	74	12	-	16.3318
216	NA	111	122	12	+	12.714
217	NA	72	83	12	-	18.363
218	NA	149	160	12	-	12.7355
219	NA	248	259	12	+	15.1813
220	NA	92	103	12	+	15.1813
221	NA	104	115	12	-	9.36516
222	NA	249	260	12	+	14.1056
223	NA	9	20	12	-	12.507
224	NA	238	249	12	+	15.5528
225	NA	128	139	12	-	14.6272
226	NA	114	125	12	+	10.714
227	NA	63	74	12	-	16.0897
228	NA	186	197	12	-	16.4899
229	NA	12	23	12	+	15.0618
230	NA	96	107	12	-	17.7204
231	NA	63	74	12	-	13.7337
232	NA	419	430	12	+	17.1891
233	NA	84	95	12	+	9.48739
234	NA	23	34	12	-	18.0782
235	NA	44	55	12	+	12.9465
236	NA	72	83	12	-	17.9766
237	NA	171	182	12	-	12.2299
238	NA	497	508	12	+	17.8694
239	NA	105	116	12	-	18.5221
240	NA	267	278	12	-	18.4591
241	NA	5	16	12	-	10.9359
241	NA	74	85	12	-	10.9359
241	NA	147	158	12	-	10.9359
242	NA	135	146	12	-	14.9139
243	NA	78	89	12	-	17.4295
244	NA	223	234	12	+	16.789
245	NA	294	305	12	-	17.9629
246	NA	204	215	12	+	15.2294
247	NA	53	64	12	-	11.7533
248	NA	57	68	12	+	19.8254
249	NA	281	292	12	+	10.6528
250	NA	192	203	12	+	13.8257
251	NA	153	164	12	-	19.8254
252	NA	264	275	12	+	17.9629
253	NA	24	35	12	+	11.2743
254	NA	33	44	12	-	16.7757
255	NA	43	54	12	-	18.4591
256	NA	166	177	12	+	17.1891
257	NA	150	161	12	+	16.4341
258	NA	193	204	12	+	17.4295
259	NA	78	89	12	-	17.7932
260	NA	172	183	12	-	12.7419
261	NA	229	240	12	-	14.4222
262	NA	163	174	12	+	18.3429
263	NA	51	62	12	+	12.8142
264	NA	59	70	12	-	18.0782
265	NA	20	31	12	-	13.9973
266	NA	6	17	12	+	11.427
267	NA	152	163	12	-	17.0396
268	NA	5	16	12	+	8.52131
269	NA	172	183	12	-	15.1136
270	NA	141	152	12	-	11.5862
271	NA	43	54	12	+	16.9516

272	NA	162	173	12	+	14.3238
273	NA	126	137	12	-	12.8411
274	NA	247	258	12	+	18.0782
275	NA	156	167	12	+	13.0487
276	NA	32	43	12	+	18.142
277	NA	132	143	12	+	18.5362
278	NA	645	656	12	+	17.6481
279	NA	184	195	12	-	14.2471
280	NA	420	431	12	+	18.3232
281	NA	761	772	12	-	14.1336
282	NA	401	412	12	-	18.5362
283	NA	12	23	12	+	16.8408
284	NA	29	40	12	-	17.1691
284	NA	132	143	12	-	17.1691
285	NA	155	166	12	-	17.4295
286	NA	155	166	12	-	18.363
287	NA	89	100	12	+	16.7842
288	NA	29	40	12	+	14.6544
289	NA	157	168	12	+	12.6984
290	NA	303	314	12	-	11.8371
291	NA	253	264	12	+	17.1558
292	NA	127	138	12	+	13.6168
293	NA	341	352	12	+	18.0782
294	NA	159	170	12	+	14.9595
295	NA	9	20	12	-	16.4069
296	NA	133	144	12	+	18.0782
296	NA	174	185	12	+	18.0782
296	NA	257	268	12	+	18.0782
297	NA	313	324	12	-	17.268
298	NA	18	29	12	-	18.4067
299	NA	89	100	12	-	17.9629
300	NA	65	76	12	+	18.3567
301	NA	76	87	12	+	11.5521
302	NA	20	31	12	-	18.6515
303	NA	176	187	12	+	7.46487
304	NA	305	316	12	-	14.2128
305	NA	55	66	12	+	14.7279
306	NA	110	121	12	-	17.8694
307	NA	111	122	12	-	16.4743
308	NA	597	608	12	+	19.7101
309	NA	77	88	12	+	16.0897
310	NA	133	144	12	-	18.0782
310	NA	219	230	12	-	18.0782

Table S4 Primers used for real-time PCR

Species	Target name	Direction	Primer sequence
Human	<i>GAPDH</i>	Forward	GGAGCGAGATCCCTCCAAAAT
		Reverse	GGCTGTTGTCATACTTCTCATGG
	<i>KLF4</i>	Forward	CAGCTTCACCTATCCGATCCG
		Reverse	GACTCCCTGCCATAGAGGAGG
	<i>ICAM-1</i>	Forward	GGTAGCAGCCGCAGTCATAA
		Reverse	GATAGGTTCAGGGAGGCGTG
	<i>VCAM-1</i>	Forward	GGGAAGATGGTCGTGATCCTT
		Reverse	TCTGGGGTGGTCTCGATTTTA
	<i>PAI-1</i>	Forward	TGAGATCAGCACCACAGAC
		Reverse	ATTGATGATGAATCTGGCTCTC
	<i>NOS3</i>	Forward	GTGGCTGGTACATGAGCACT
		Reverse	TGGCTAGCTGGTAACTGTGC
	<i>THBD</i>	Forward	ACCTTCCTCAATGCCAGTCAG
		Reverse	CGTCGCCGTTTCAGTAGCAA
Mouse	<i>Actb</i>	Forward	GTGACGTTGACATCCGTAAAGA
		Reverse	GCCGGACTCATCGTACTCC
	<i>Icam-1</i>	Forward	GTGATGCTCAGGTATCCATCCA
		Reverse	CACAGTTCTCAAAGCACAGCG
	<i>Vcam-1</i>	Forward	TGGTCGCGGTCTTGGGAGCCT
		Reverse	CCGGCTTCCCAACCTCCAGGGG
	<i>Pai-1</i>	Forward	GACACCCTCAGCATGTTTCATC
		Reverse	AGGGTTGCACTAAACATGTCAG
	<i>Vegfa</i>	Forward	CTGGACCCTGGCTTTACTGC
		Reverse	CTGCTCTCCTTCTGTCTGG
	<i>Klf4</i>	Forward	GAAGGTCGTGGCCCCGAAA
		Reverse	TCAGTTCATCGGAGCGGGCG

Supplementary figure legends

Figure S1 | TA-TMA patients exhibit abnormal complement activation and endothelial injury.

A-C, C3b (A), C5b-9 (B), and KLF4 (C) levels across: TA-TMA patients (n = 20), controls (n = 20), acute graft-versus-host disease (aGVHD) patients (n = 10), and infection groups (n = 10).

D, Endothelial progenitor cells (EPCs) and mature circulating endothelial cells (mCECs) in peripheral blood in TA-TMA patients and controls are defined by flow cytometry. Bar graphs show the quantification of EPCs and mCECs. n = 10 per group.

E, Activated CECs (aCECs) and resting CECs (rCECs) in TA-TMA patients and controls are determined by flow cytometry and the bar graphs show the quantification of aCECs and rCECs. n = 10 per group.

p < 0.01, *p < 0.001, ****p < 0.0001. ns, not significant.

Figure S2 | Upregulation of KLF4 attenuates complement deposition and endothelial injury induced by TA-TMA plasma.

A, Complement C3 levels were determined by flow cytometry, and the bar graph shows fluorescence intensity of complement C3 on the HUVECs surface after incubation with plasma from control, infection, aGVHD and TA-TMA patients.

B, C, Flow cytometric analysis of C3 (B) and C5b-9 (C) deposition on HUVECs exposed to control plasma, TA-TMA plasma, or TA-TMA plasma supplemented with different concentrations of APTO253 (1 μ M, 10 μ M, 100 μ M). Bar graphs show mean fluorescence

intensities.

D, Western blot shows enhanced KLF4 expression in HUVECs treated with 10 μ M APTO253. Bar graph shows relative intensity of KLF4.

E, Western blot of C3, C5, C4, CFB, MBL2, and C1QA in HUVECs exposed to control plasma, TA-TMA plasma, or TA-TMA plasma supplemented with 10 μ M APTO253. Bar graphs show relative protein levels.

F, Immunofluorescence staining of C3, C5b-9, C5, C4, CFB, MBL2, and C1QA in HUVECs under the same treatments. The bar graphs show mean fluorescence intensities. Scale bars: 50 μ m.

G–K, qPCR analysis of *ICAM-1* (G), *VCAM-1* (H), *PAI-1* (I), *NOS3* (J), and *THBD* (K) in corresponding groups.

The results are representatives of three experiments. * $p < 0.05$, ** $p < 0.01$, *** $p < 0.001$, **** $p < 0.0001$. ns, not significant.

Figure S3 | KLF4 overexpression reduces complement deposition and endothelial injury under TA-TMA plasma challenge.

A, Flow cytometric assessment of lentiviral transduction efficiency for control (PCDH) and KLF4-overexpressing (OEKLF4) vectors.

B, C, qPCR (B) and Western blot (C) confirming elevated KLF4 mRNA and protein levels in OEKLF4-transduced HUVECs.

D-F, Bar graphs compare the relative intensities of CFB (D), MBL2 (E) and C1QA (F) in PCDH and OEKLF4 cells treated with control or TA-TMA plasma.

G, Immunofluorescence analysis of the complement components (C3, C5b-9, C5, C4, CFB, MBL2, C1QA) in these cells. Scale bars: 50 μ m.

H–L, Relative mRNA levels of *ICAM-1* (H), *VCAM-1* (I), *PAI-1* (J), *NOS3* (K), and *THBD* (L) determined by qPCR.

The results are representatives of three experiments. * $p < 0.05$, ** $p < 0.01$, *** $p < 0.001$, **** $p < 0.0001$. ns, not significant.

Figure S4 | KLF4 activates CD46 transcription in HUVECs.

A–D, KLF4-overexpressing (OEKLF4) and control lentiviral-transduced cells (PCDH) were incubated with TA-TMA plasma for 12 h and subjected to CUT&Tag assay with an anti-KLF4 antibody. A-B, the heatmap showed the distribution of KLF4 peaks in the vicinity of the translation start site (TSS). C, Annotation of KLF4 peaks on the genome. D, KEGG analysis of KLF4-enriched peaks in promoter regions.

E–G, RNA-seq analysis comparing OEKLF4 to PCDH cells under TA-TMA plasma for 12 h. E, Volcano plot of differentially expressed genes (DEGs). F, KEGG pathway analysis of upregulated genes. G, Overlap of CUT&Tag and RNA-seq data identifies potential KLF4 targets.

H, I, *CD46* mRNA levels measured by qPCR in OEKLF4 and PCDH cells exposed to acute graft-versus-host-disease plasma (H) and infection plasma (I). The results are representatives of three experiments.

J, Western blot validating stable CD46 knockdown (ShCD46) in HUVECs. The results are representatives of three experiments.

K-M, The bar graphs indicate the relative intensities of C4 (K), CFB (L) and MBL2 (M) in ShCD46 or control cells (PLKO.1) treated with control plasma, TA-TMA plasma, or TA-TMA plasma plus APTO253.

*p < 0.05, ** p < 0.01. ns, not significant.

Figure S5 | Upregulation of KLF4 attenuates the TA-TMA phenotype in mice.

A, Schematic timeline of APTO253 administration in the TA-TMA mouse model.

B, Western blot analysis of KLF4 levels in renal tissues from DMSO- and APTO253-treated mice. Bar graph shows relative intensity of KLF4. n = 4.

C, Hemoglobin (HGB) levels and platelet counts in mice treated with APTO253 or DMSO.

D, Representative peripheral blood smears ($\times 100$) showing fewer schistocytes (arrows) in the APTO253 group. Scale bars: 10 μm .

E–G, Plasma lactate dehydrogenase (LDH) (E), blood urea nitrogen (BUN) (F), and sC5b-9 (G).

H, Representative hematoxylin & eosin (H&E) and periodic acid–Schiff (PAS) staining highlighting improved glomerular architecture in the APTO253 group. Scale bar: 10 μm .

Pound sign (#) indicates congestion; asterisk (★) indicates endothelial swelling/detachment.

I, Immunofluorescence of C3 and C5b-9 in renal sections. Bar graphs show mean fluorescence intensities. Scale bars: 10 μm .

J-M, qPCR quantification of *Icam-1* (J), *Vcam-1* (K), *Pai-1* (L), and *Vegfa* (M) in renal tissue.

n = 4.

N-P, Plasma ICAM-1 (N), VCAM-1 (O), and PAI-1 (P).

Q, Kaplan–Meier survival curves for mice receiving different treatments.

The results are representatives of three experiments and six mice/group unless indicated.

*p < 0.05, **p < 0.01, ***p < 0.001, ****p < 0.0001. ns, not significant.

Figure S6 | In vivo KLF4 overexpression attenuates TA-TMA pathology.

A, Illustration of the protocol for KLF4 overexpression.

B, C, qPCR (B) and Western blot (C) analyses showing elevated KLF4 levels in renal tissues of mice receiving mKLF4 plasmids compared with vector controls. n = 4.

D-E, Plasma BUN (D) and sC5b-9 (E) in the indicated groups.

F-I, Relative mRNA levels of *Icam-1* (F), *Vcam-1* (G), *Pai-1* (H), and *Vegfa* (I) in renal tissue.

n = 4.

J-L, Plasma levels of ICAM-1 (J), VCAM-1 (K), and PAI-1 (L).

The results are representatives of three experiments and six mice/group unless indicated.

*p < 0.05, **p < 0.01, ***p < 0.001, ****p < 0.0001.

Figure S7 | Statin treatment ameliorates TA-TMA by upregulating KLF4.

A, Timeline outlining pravastatin administration.

B, Western blot analysis of KLF4 levels in renal tissues from mice treated with pravastatin or vehicle. Bar graph shows relative intensity of KLF4. n = 4.

C-D, Plasma BUN (C) and sC5b-9 (D) in each group.

E-H, qPCR of *Icam-1* (E), *Vcam-1* (F), *Pai-1* (G), and *Vegfa* (H) in renal tissue. n = 4.

I-K, Plasma ICAM-1 (I), VCAM-1 (J), and PAI-1 (K) levels.

The results are representatives of three experiments and six mice/group unless indicated.

* $p < 0.05$, ** $p < 0.01$, *** $p < 0.001$.

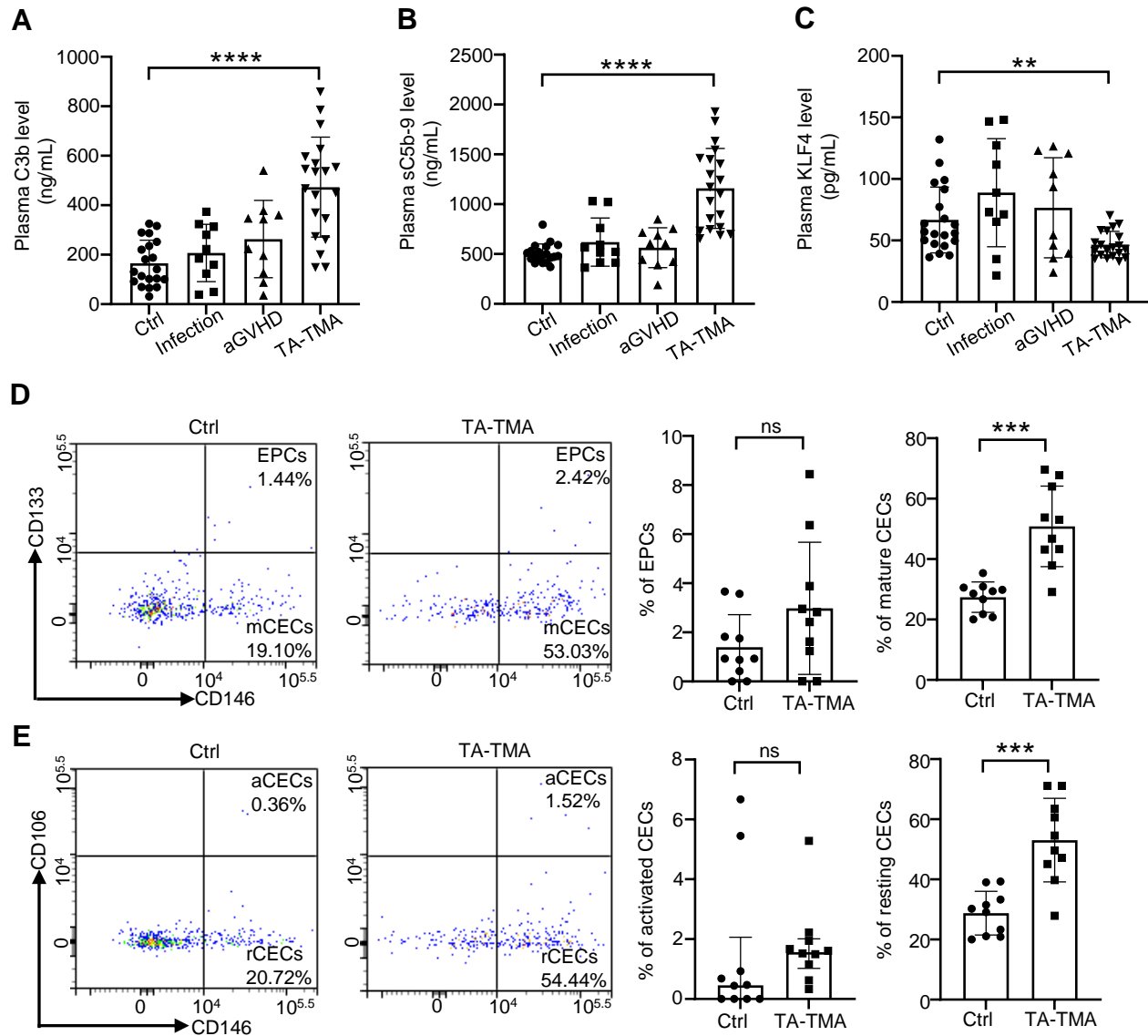
Figure S1

Figure S2

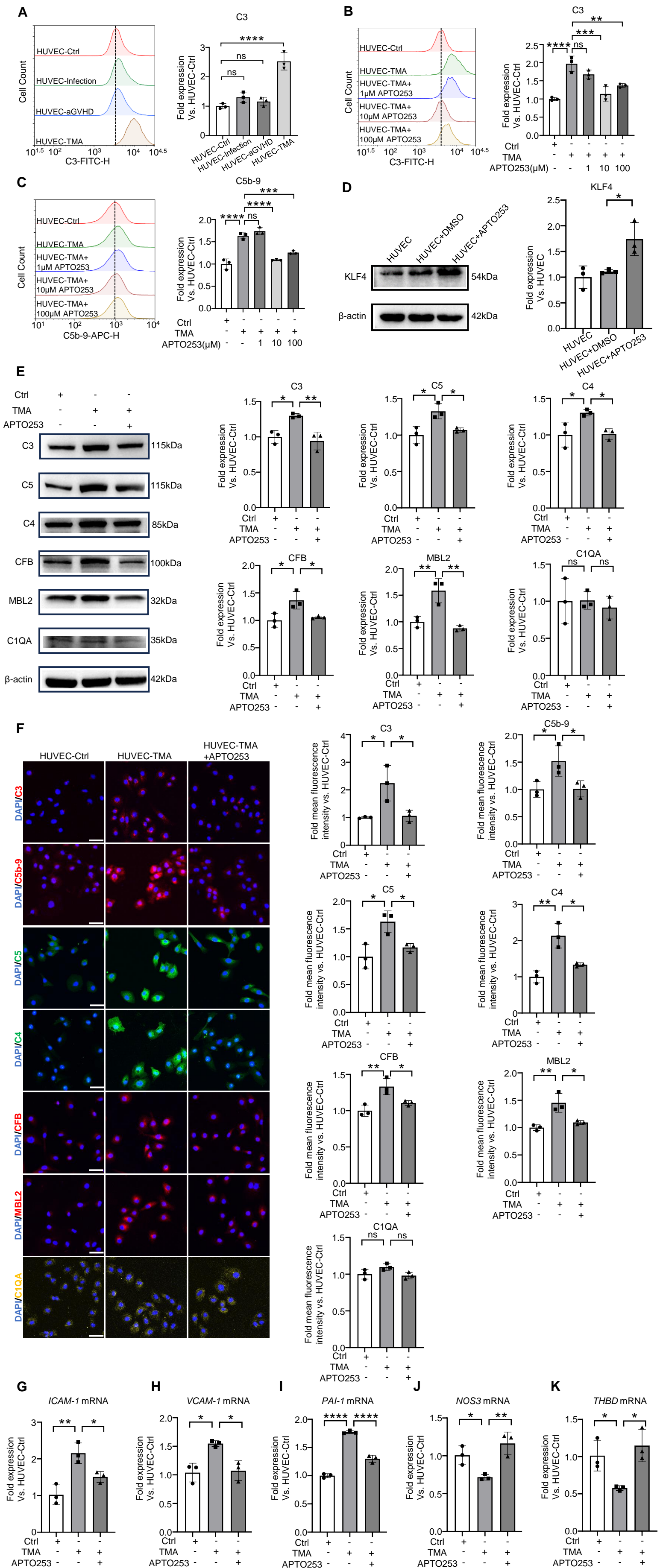
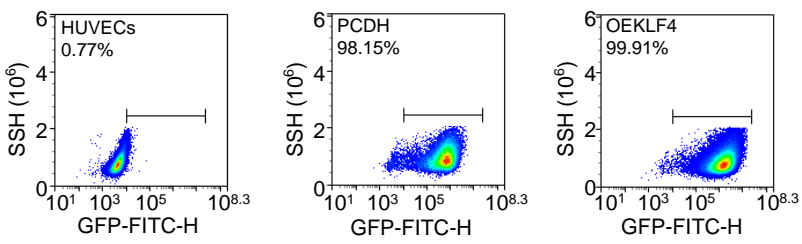
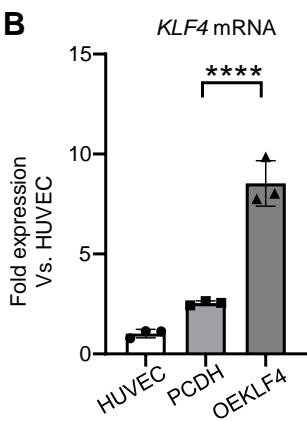


Figure S3

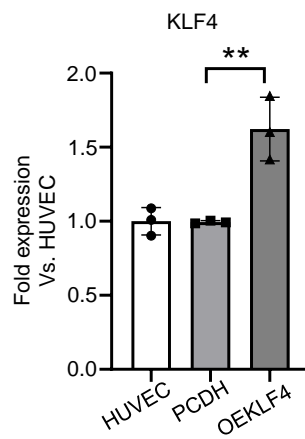
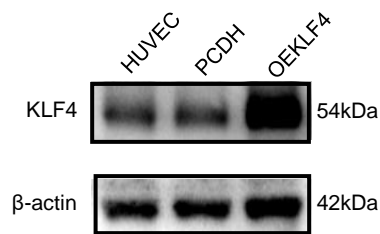
A



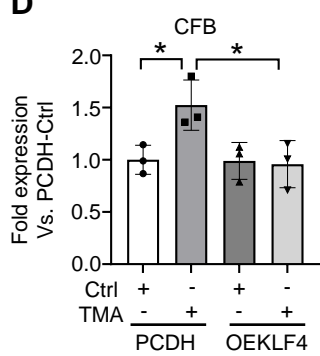
B



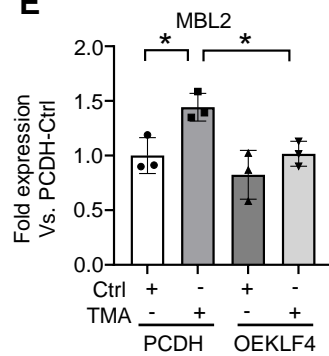
C



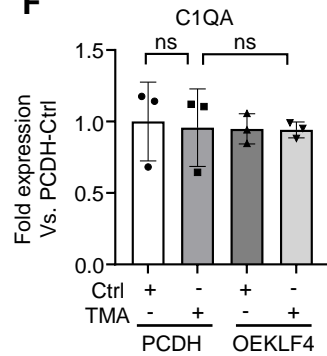
D



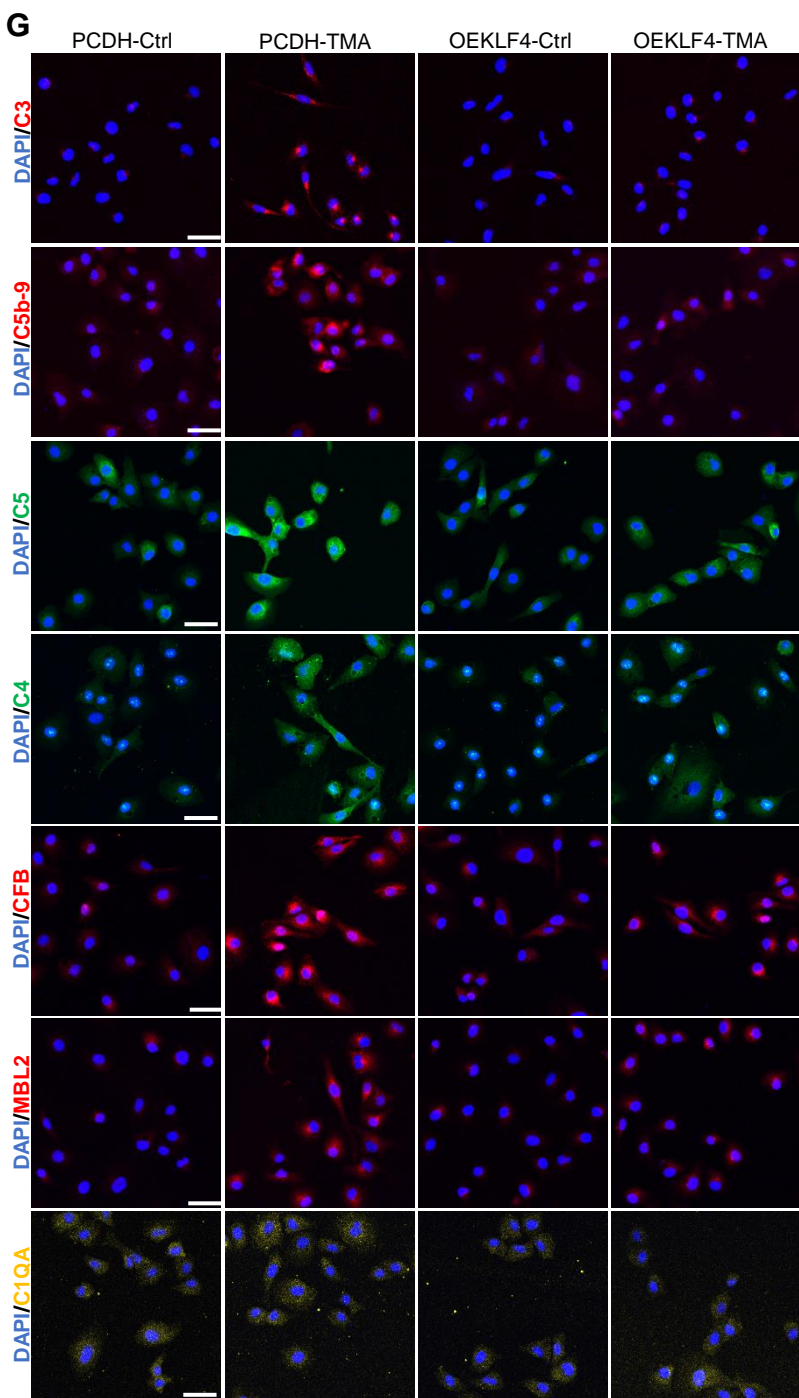
E



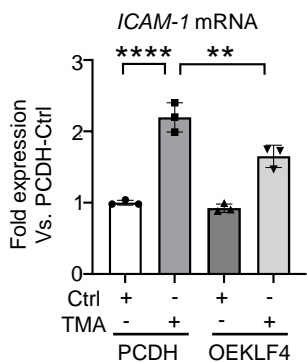
F



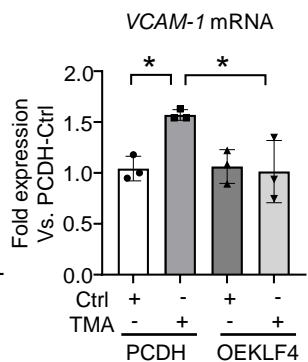
G



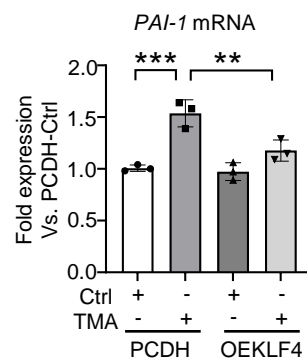
H



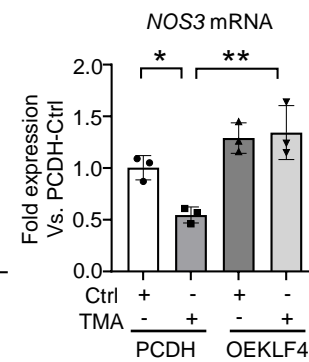
I



J



K



L

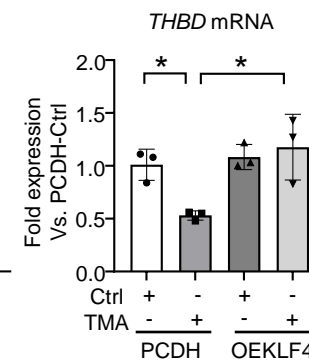


Figure S4

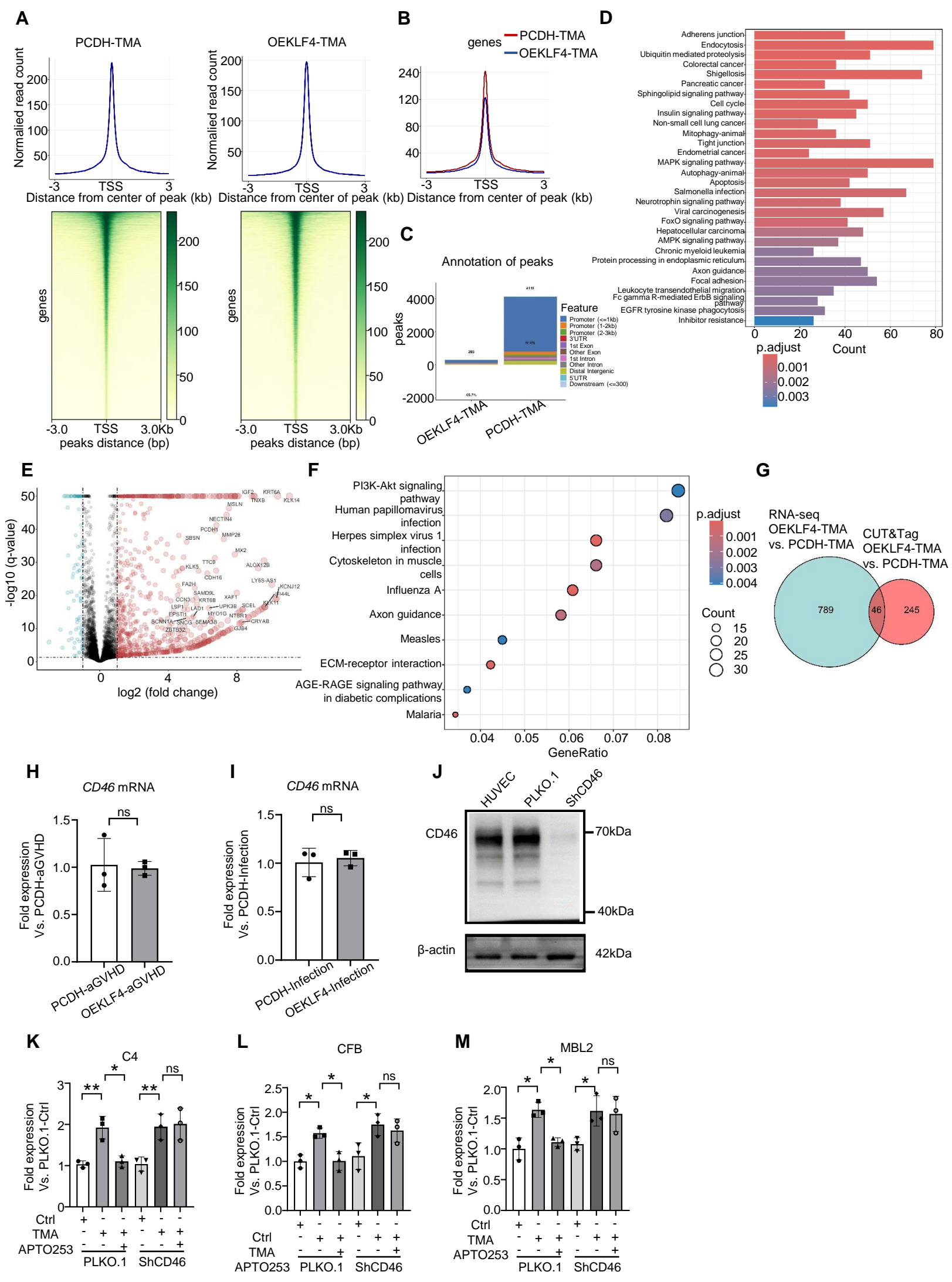


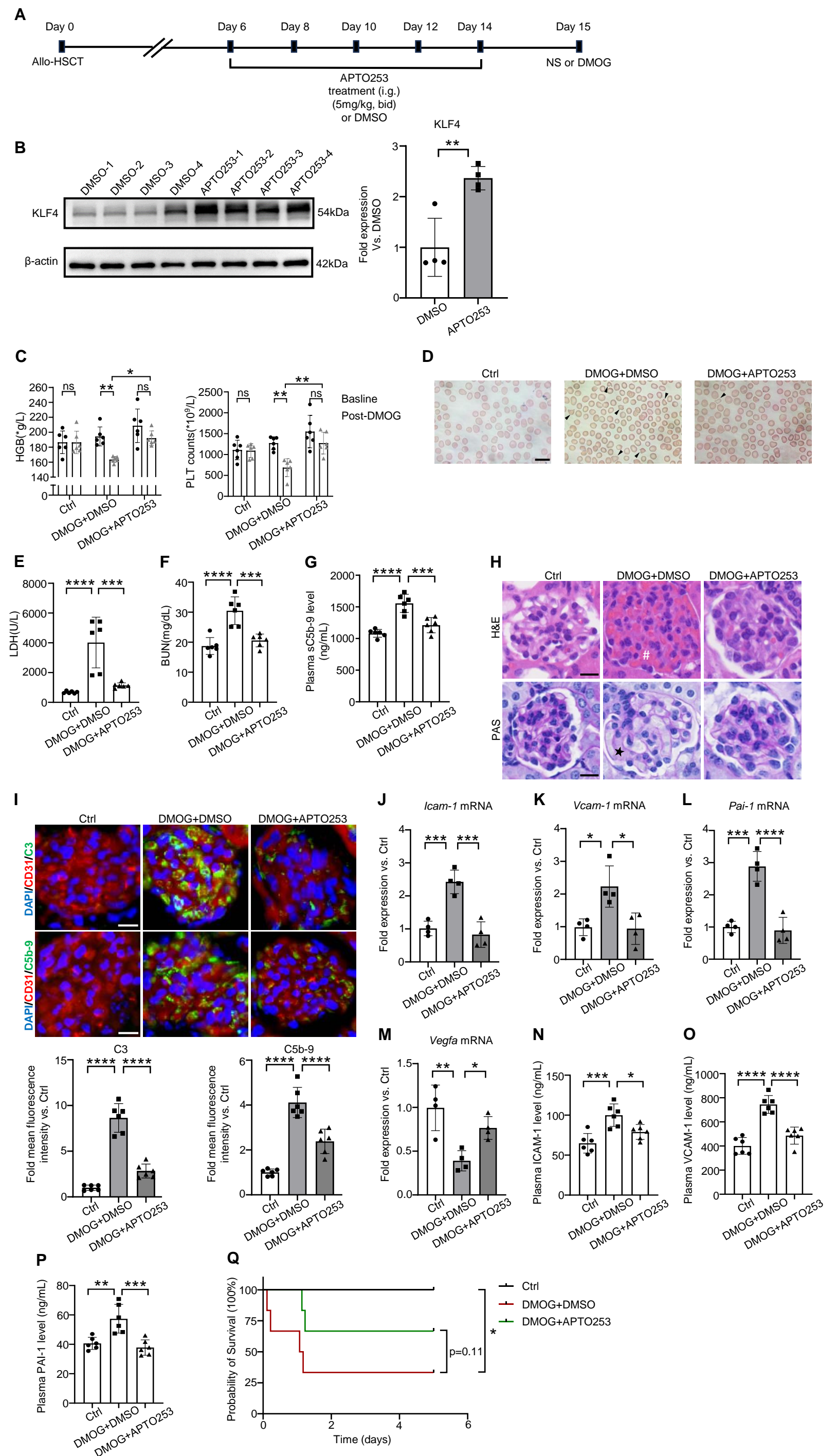
Figure S5

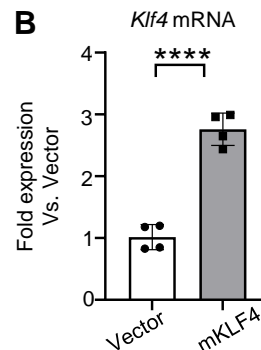
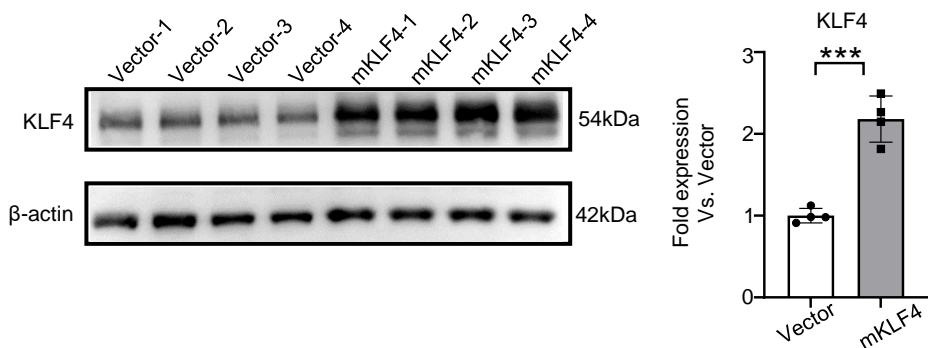
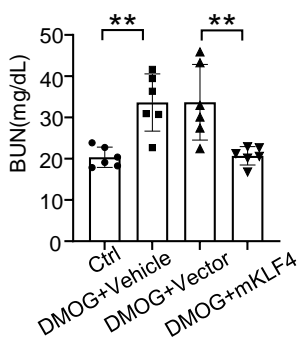
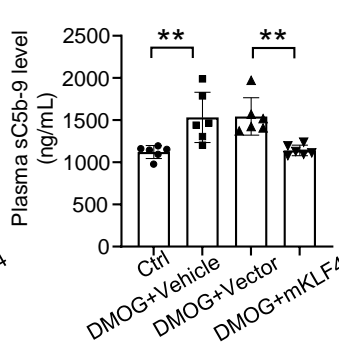
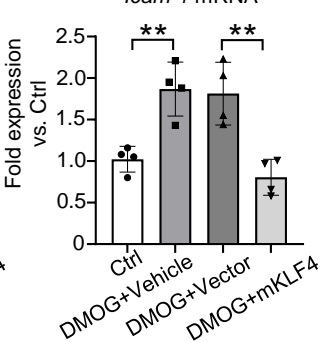
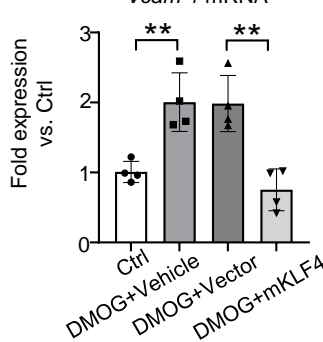
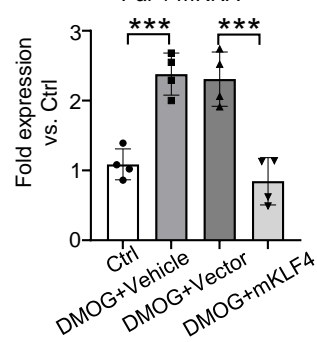
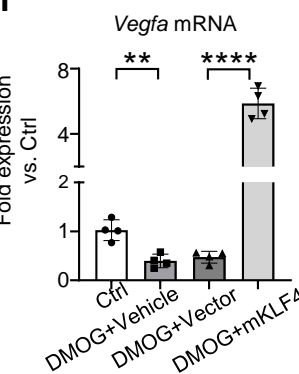
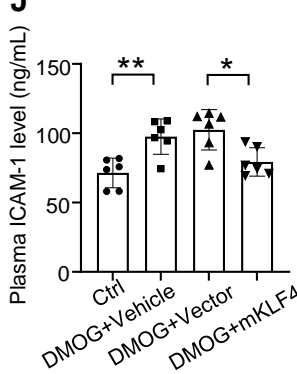
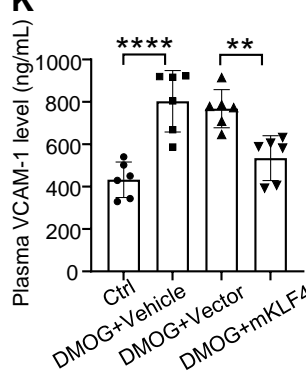
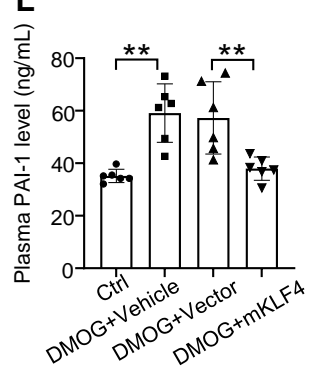
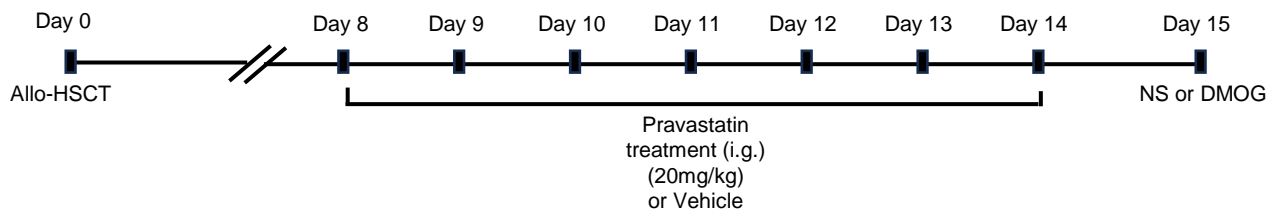
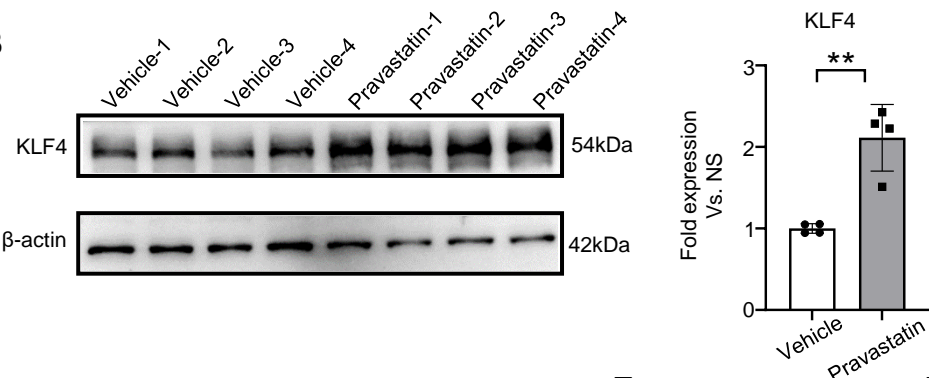
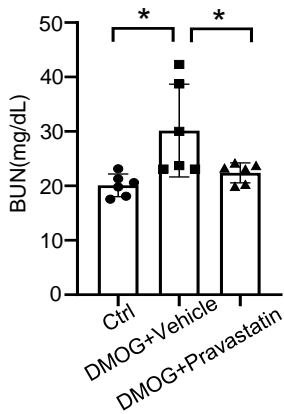
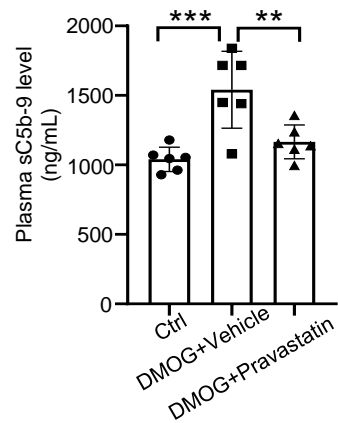
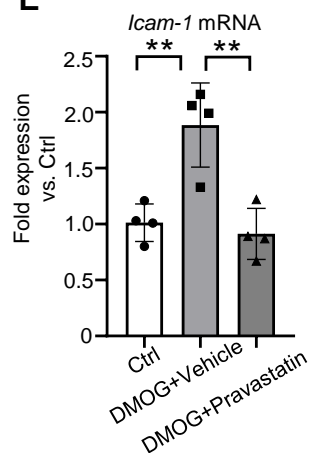
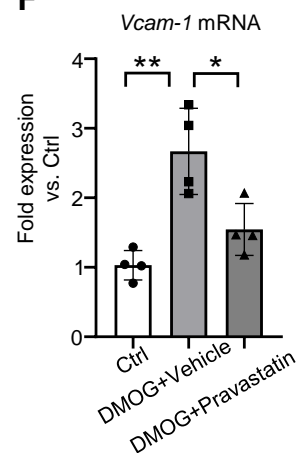
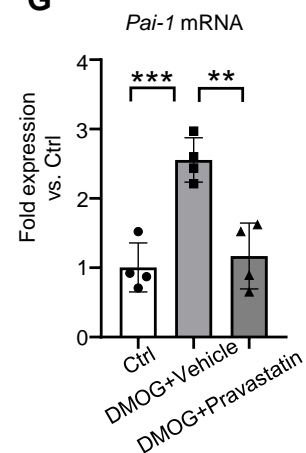
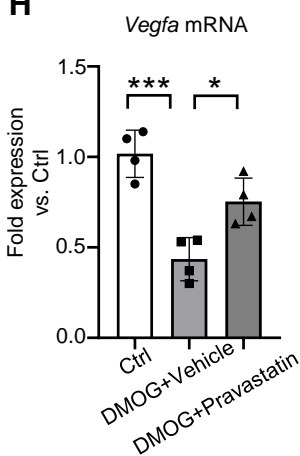
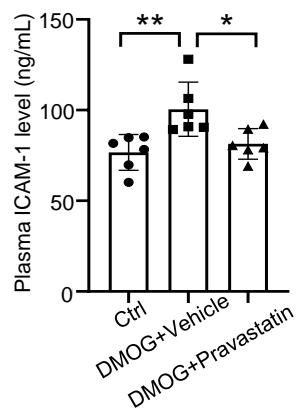
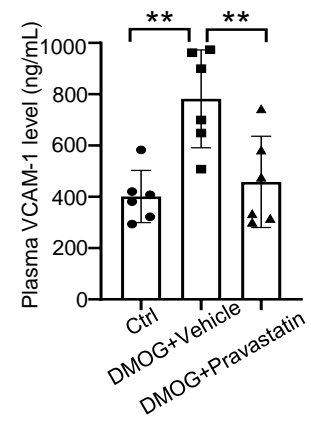
Figure S6**A****B****C****D****E****F****G****H****I****J****K****L**

Figure S7**A****B****C****D****E****F****G****H****I****J****K**